Journal of The Electrochemical Society, **157** (2) D81-D84 (2010)
0013-4651/2009/157(2)/D81/4/$28.00 © The Electrochemical Society

Characterization and Growth Kinetics of Electroless Pure Nickel Thin Films on Si(001) Substrates

S. L. Cheng[z] **and H. C. Peng**

Department of Chemical and Materials Engineering, National Central University, Chung-Li City, Taoyuan 32001, Taiwan

We report the results on the growth behaviors of electroless pure nickel thin films on Si(001) substrates from a systematic investigation. Continuous pure Ni films with a polycrystalline structure were successfully plated on the surfaces of Si substrates using the hydrazine-modified electroless Ni deposition processes. The thicknesses of the pure Ni films can be controlled by tuning the electroless plating temperature and time. The deposition rate of the electroless pure Ni films increased exponentially with the plating temperatures. The activation energy of the electroless pure Ni deposition on Si(001) substrate for samples plated at 55–75°C could be calculated from an Arrhenius plot, and it was about 0.95 eV/atom.
 [DOI: 10.1149/1.3263266]

Manuscript submitted September 2, 2009; revised manuscript received October 18, 2009. Published December 7, 2009.

Compared with the conventional vacuum deposition methods, such as thermal and E-beam evaporations, sputtering, and chemical vapor deposition, electroless wet-chemical plating offers a relatively facile, low cost, and efficient technique for the deposition of desired metal and alloy layers onto the surfaces of conducting and nonconducting engineering components with complex geometries.[1,2] During the past decades, the wet-chemical deposition of metallic films by electroless plating has been widely used in many industries, especially in the production of hard coatings to protect the engineering components from oxidation and degradation caused by wear and corrosion.[3-6] Among the variety of electroless metallic coatings, electroless nickel-based films are perhaps the most versatile materials used in engineering due to their unique magnetic and mechanical properties, as well as good thermal and chemical stabilities.[7-10]

In addition to the production of protective coatings, many recent research efforts have been dedicated to the integration of electroless Ni plating process into the fabrication of electrical contacts and interconnects in microelectronic and optoelectronic devices.[11-14] However, in these studies, borohydride, dimethylamine borane, or hypophosphite was usually utilized as the chemical reducing agents, leading to the incorporation of a significant amount of impurities (e.g., boron or phosphorus) in the electroless Ni layers. Several previous studies have demonstrated that these impurities would lead to an increase in the electrical resistivity and decrease in the crystallinity and solderability of the deposited Ni films.[15-17] These drawbacks could limit practical applications of electroless Ni in microelectronics and packaging. To overcome the aforementioned limitations, an alternative and effective synthesis route, which is based on the hydrazine-modified electroless pure Ni deposition process, has recently been developed.[18-20] Although the improved electroless plating method using hydrazine as the reducing agent has successfully been applied to produce pure Ni film and nanostructure,[19,21,22] the corresponding studies on the growth kinetics of electroless pure Ni deposition on Si substrates are relatively scarce. Because the kinetic data are crucial for a fundamental understanding of the electroless pure Ni plating process and for a reliable parameter estimation, it is important to investigate them further under different experimental conditions.

In this study, we report the results of a cross-sectional transmission electron microscopy (XTEM) investigation of the growth kinetics of electroless pure nickel thin films on Si(001) substrates. The microstructures, crystallinities, and chemical compositions of the electroless nickel films produced at various synthesis temperatures and time are studied.

Experimental

Single-crystal, 1–100 Ω cm, boron-doped Si(001) wafers were used as the deposition substrates in the present study. The Si(001) wafers were cut into pieces of about 1×0.5 cm^2. All of these Si substrates were chemically cleaned by a standard procedure and then dipped in a dilute HF solution ($HF:H_2O = 1:50$) to remove the native oxide layer. Before the electroless Ni plating process, the cleaned Si surfaces were presensitized by dipping the substrates in a solution containing 70 g/L stannous chloride ($SnCl_2 \cdot 2H_2O$) and 70 mL/L hydrochloric acid (HCl) for 2 min and rinsed with deionized (DI) water. Then the sensitized Si substrates were treated with a solution of 0.3 g/L palladium chloride ($PdCl_2$) and 6.25 mL/L HCl for 1 min at room temperature to activate the surface of the Si substrates. Subsequently, the electroless pure Ni deposition process was carried out by immersing the Pd-activated Si substrates into the electroless nickel plating baths at 55–75°C for various plating time. The electroless Ni plating solution was composed of 0.005 M nickel sulfate ($NiSO_4 \cdot 6H_2O$) as the Ni metal source and 0.25 M hydrazine ($N_2H_4 \cdot H_2O$) as the chemical reducing agent. The pH value of the Ni plating solution was monitored and controlled at 11.5 ± 0.1 by the addition of ammonium hydroxide (NH_4OH) solution. After the electroless deposition process, the obtained samples were thoroughly washed with DI water and blown dry with N_2 gas.

The surface morphologies of the as-activated samples and as-synthesized Ni metal films were examined using scanning electron microscopy (SEM). Plan-view transmission electron microscopy (TEM) and selected area electron diffraction (SAED) analysis were carried out for microstructure examination and crystallography characterization. The thicknesses of the Ni metal films deposited on Si(001) substrates at various reaction temperatures and times were determined by XTEM. Most of the XTEM micrographs were taken along the [110] zone axis of the single-crystal Si. Link ISIS energy dispersion spectrometers (EDSs) attached to the SEM and TEM were utilized to determine the chemical compositions of local areas in the samples.

Results and Discussion

Figure 1a shows a typical plan-view SEM micrograph of the Si(001) substrate after the Sn sensitization and Pd activation treatments. As can be seen in Fig. 1a, dense nanoparticles, several nanometers in size, were found to form and disperse on the surface of the silicon substrate. From the EDS analysis, it is evident that these nanoparticles produced were found to be composed of pure palladium. The corresponding EDS spectrum of the Pd nanoparticles is shown in the upper right inset of Fig. 1a. The Pd nanoparticles were then served as the catalysts in the following electroless nickel plating process. Figure 1b and c shows the photographs of the Pd-activated Si substrates before and after electroless Ni deposition, respectively, using hydrazine as the reducing agent. As can be seen from the photographs, the as-deposited electroless Ni film exhibits a bright metal color. The observed bright color suggests that the Ni film produced was composed of fine grains and its surface morphology was flat. A representative XTEM micrograph of the electroless

[z] E-mail: slcheng@ncu.edu.tw

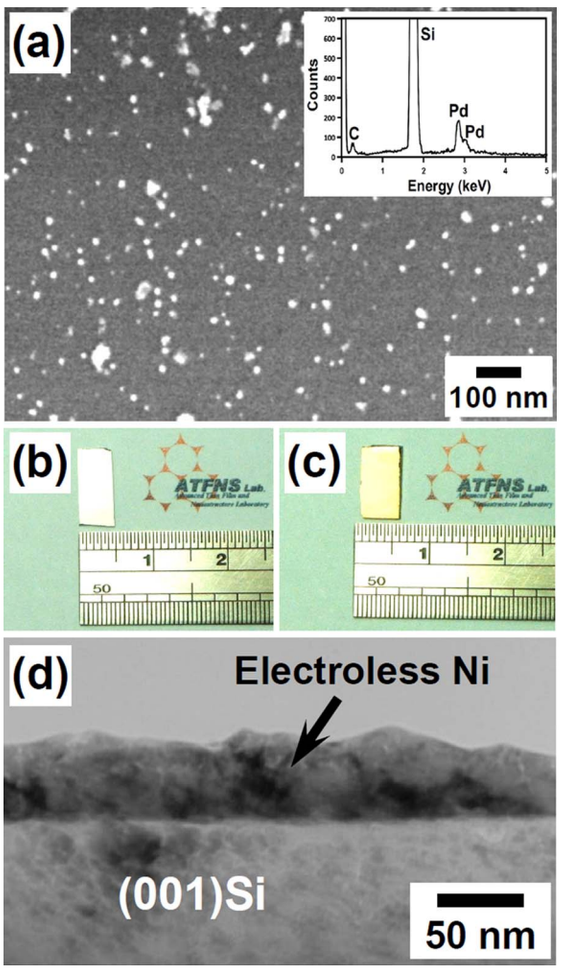

Figure 1. (Color online) (a) A typical plan-view SEM micrograph of the Si(001) substrate after the Sn sensitization and Pd activation treatments. The inset is the corresponding EDS spectrum of the nanoparticles. Photographs of the Pd-activated Si substrates (b) before and (c) after the electroless deposition of pure Ni thin films. (d) A representative bright-field XTEM micrograph of an as-deposited electroless pure Ni film on Si(001) substrate.

nickel deposited on Si(001) substrate is shown in Fig. 1d. For the samples plated at various temperatures and time, the surface morphologies, crystallinities, and chemical compositions of the electroless nickel films were further examined by SEM, TEM, EDS, and SAED analyses.

Figure 2a-d shows the plan-view SEM micrographs of Ni films plated at 65°C for 5–11 min and at 75°C for 3–5 min, respectively. As seen in Fig. 2, it is obvious that an increase in the electroless plating temperatures and time leads to a gradual increase in grain sizes of the electrolessly deposited Ni films. Some of the Ni grains produced at a higher temperature or at a longer time exhibit faceted surface morphologies. Similar trends for the electroless deposition of other metallic layers were reported in previous literatures.[23,24] Figure 3a and b shows a typical XTEM micrograph and the corresponding EDS spectrum of an electroless Ni film, respectively. The EDS analysis clearly demonstrated that the electroless film produced was entirely composed of pure nickel. The appearance of Cu peak in the EDS spectrum is attributed to the copper grid used for supporting the TEM specimen. The microstructures and crystallinities of the produced Ni films were investigated in more detail by plan-view TEM and SAED analysis. Representative TEM micrographs and the corresponding SAED pattern of the as-deposited Ni film are shown in Fig. 4a and b, respectively. From the SAED analysis, diffraction

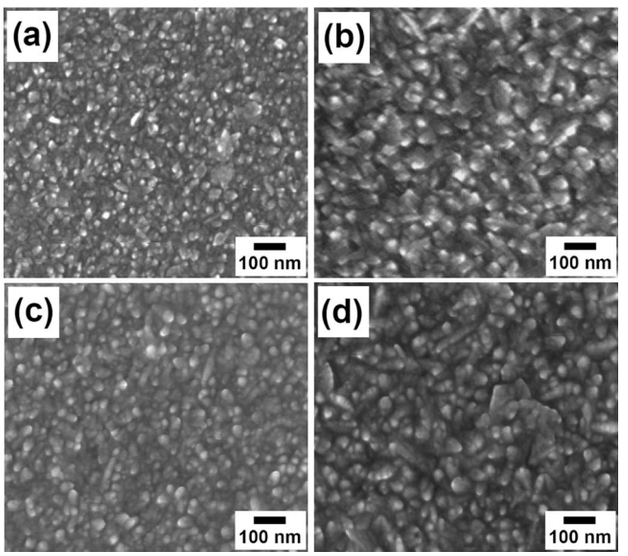

Figure 2. Plan-view SEM micrographs of electroless pure Ni films deposited at 65°C for (a) 5 and (b) 11 min, and at 75°C for (c) 3 and (d) 5 min.

rings corresponding to the (111), (200), (220), (311), and (222) diffractions of pure Ni phase were detected in the electron diffraction pattern, indicating that the electroless Ni films were polycrystalline with a pure face-centered cubic structure. Moreover, from the bright- and dark-field plan-view TEM micrographs, as shown in Fig. 4a, an equiaxial grain structure can clearly be seen and the typical grain size of the polycrystalline pure Ni film was measured to be in the range of 30–80 nm.

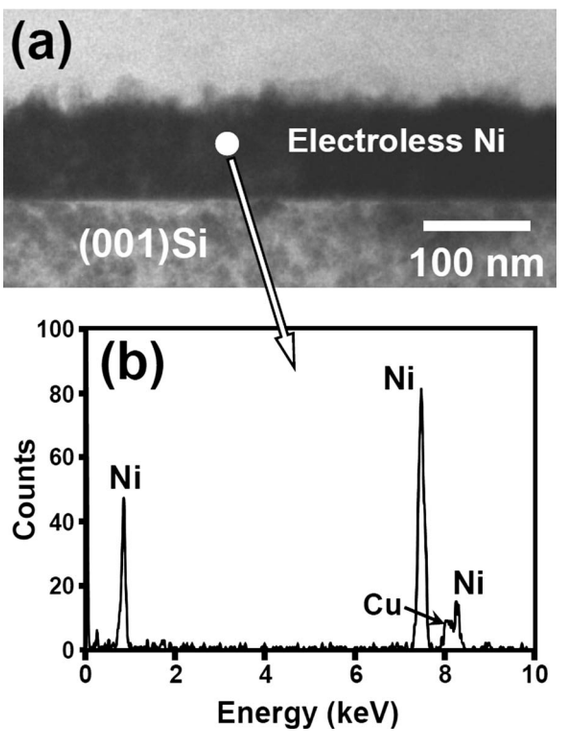

Figure 3. (a) Bright-field XTEM micrograph and (b) the corresponding EDS spectrum of the electroless pure Ni film on Si(001) deposited at 70°C for 9 min.

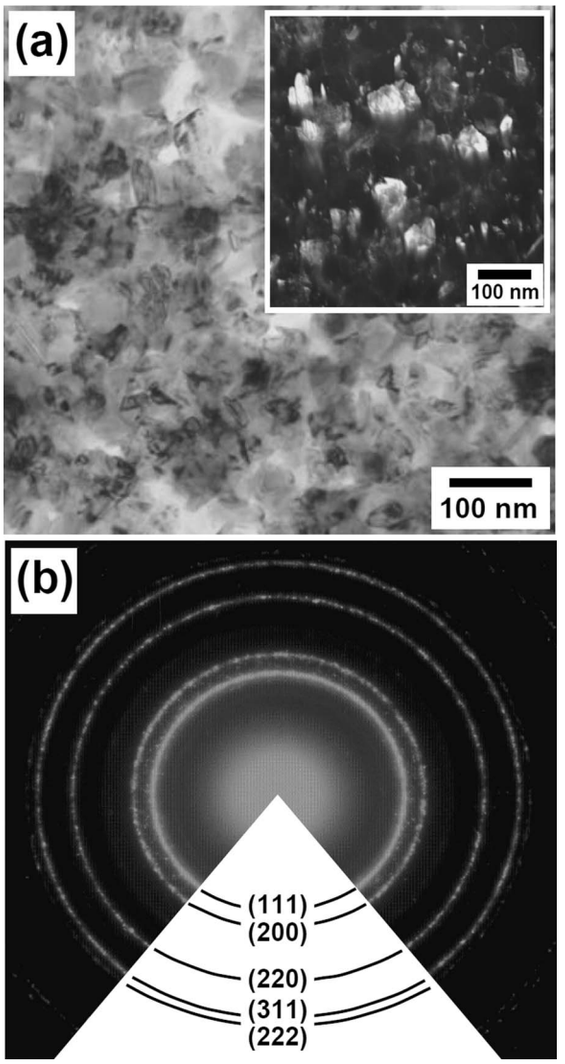

Figure 4. (a) Bright-field plan-view TEM micrograph and (b) the corresponding indexed SAED pattern of the electroless pure Ni film deposited at 70°C for 9 min. The inset in (a) is the corresponding dark-field TEM micrograph.

Figure 5a-c and d-f shows the XTEM micrographs of pure Ni thin films plated at 60°C for 9–13 min and at 70°C for 5–9 min, respectively. The TEM observations clearly revealed that all the plated Ni films were dense and continuous and the interfaces between electroless Ni films and Si substrates were relatively smooth. The thicknesses of the produced pure Ni films increase with electroless plating temperatures and time, ranging from 35 to 95 nm. Similar electroless deposition behaviors were also observed for other Si substrates plated at 55, 65, and 75°C for various periods of time in this study. After a series of XTEM examinations, the thicknesses of the electroless pure Ni films vs deposition time data for Si(001) substrates plated at temperatures from 55 to 75°C were obtained, as shown in Fig. 6a. The relation curves shown in Fig. 6a are almost linear. The result indicates that in the range of plating temperatures and time studied, the growth of electroless Ni films on Si is reaction-controlled. From the slopes of the straight lines presented in Fig. 6a, the average Ni deposition rates at various temperatures could be readily estimated. An example is shown in Fig. 6b. Furthermore, as can be seen in Fig. 6b, the plating rate of the electroless pure Ni deposition increases exponentially with the plating temperatures from 2.7 to 19.4 nm/min.

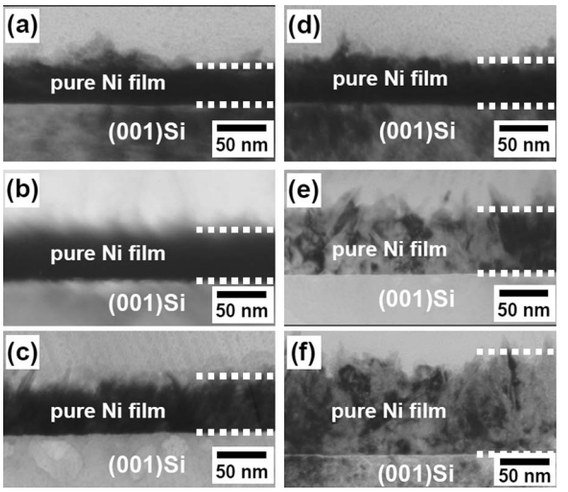

Figure 5. Bright-field XTEM micrographs of electroless pure Ni thin films deposited at 60°C for (a) 9, (b) 11, and (c) 13 min, and at 70°C for (d) 5, (e) 7, and (f) 9 min.

By measuring the Ni plating rate at different deposition temperatures, the activation energy, E_a, of the electroless pure Ni deposition can be determined using the Arrhenius relationship

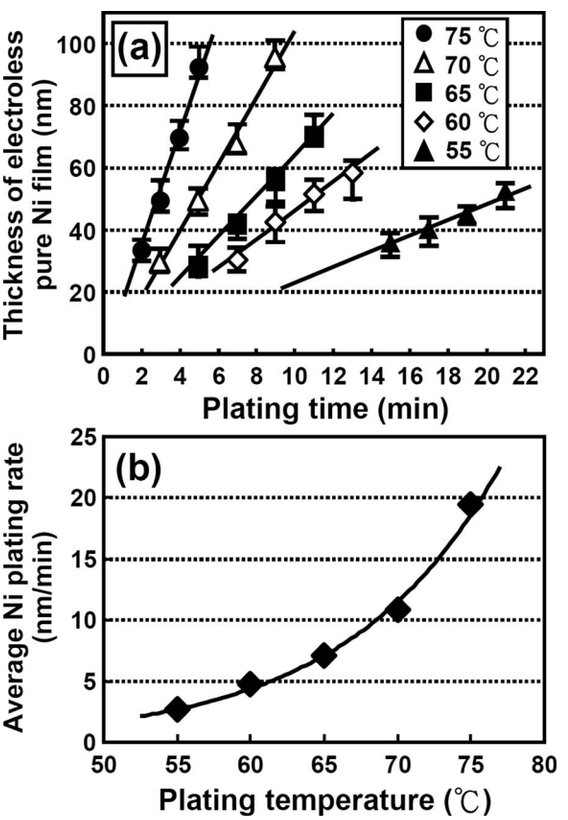

Figure 6. (a) Thickness of the electroless pure Ni film vs the electroless plating time curves for the Si(001) substrates plated at different temperatures. (b) The average electroless pure Ni plating rate as a function of electroless plating temperature.

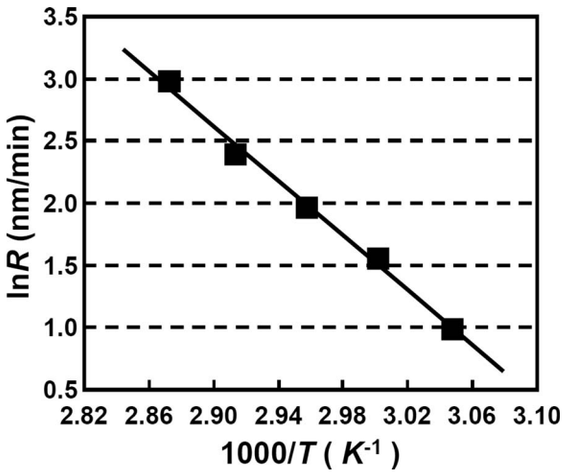

Figure 7. Arrhenius plot of the electroless plating rate vs the reciprocal of the plating temperature for the electroless deposition of pure Ni thin films on Si(001) substrates.

$$R = A \exp(-E_a/kT) \quad [1]$$

where R is the plating rate, A is the rate constant, and k and T are the Boltzmann constant and absolute temperature, respectively. The nature logarithmic value of the plating rate ($\ln R$) is plotted vs the reciprocal of the absolute temperature ($1/T$) as shown in Fig. 7. The activation energy of the electroless pure Ni deposition on Si(001) substrate can then be calculated from the slope of Fig. 7, and it was about 0.95 eV/atom. Compared with the reported data, this obtained activation energy value is in the same order of magnitude as that reported in previous literatures for different electroless plating electrolytes. For examples, Liu et al. reported that the activation energies of the electroless Ni–P films deposition on Si(001) and Fe/Si substrates were 0.71–0.82 eV/atom (68.8–79.4 kJ/mole) and 0.43–1.03 eV/atom (68.8–79.4 kJ/mole), respectively,[24,25] and Wehner et al. also reported an activation energy of 1.33 ± 0.1 eV/atom (128 ± 10 kJ/mole) for electroless-plated Ni–B films on copper substrates.[26]

Conclusions

In summary, the present study has demonstrated that dense and continuous pure Ni thin films were successfully plated on Si(001) substrates by using the hydrazine-modified electroless Ni deposition processes. The growth kinetics, surface morphologies, crystal structures, and chemical compositions of the electroless nickel films produced at various temperatures and times have been investigated.

The grain sizes of the electrolessly deposited Ni films gradually increase with increasing electroless plating temperatures and times. From TEM, SAED, and EDS analyses, it can be concluded that the electroless film produced was entirely composed of pure nickel and its crystal structure was polycrystalline. The thicknesses of the electroless pure Ni films increase linearly with the deposition time for silicon substrates plated at 55–75°C. By measuring the Ni plating rate at different temperatures, the activation energy for the linear growth of the electroless pure Ni films on blank Si(001) was derived from an Arrhenius plot to be about 0.95 eV/atom.

Acknowledgment

The research was supported by the National Science Council of Taiwan.

National Central University assisted in meeting the publication costs of this article.

References

1. T. Osaka, T. Homma, and K. Inoue, *J. Electrochem. Soc.*, **138**, 538 (1991).
2. M. Okumiya, Y. Tsunekawa, T. Saida, and R. Ichino, *Surf. Coat. Technol.*, **169–170**, 112 (2003).
3. M. Schlesinger, X. Y. Meng, and D. D. Snyder, *J. Electrochem. Soc.*, **138**, 406 (1991).
4. T. Mimani and S. M. Mayanna, *Surf. Coat. Technol.*, **79**, 246 (1996).
5. K. M. Gorbunova, M. V. Ivanov, and V. P. Moiseev, *J. Electrochem. Soc.*, **120**, 613 (1973).
6. M. Menningen, H. Weiss, and U. Fischer, *Surf. Coat. Technol.*, **71**, 208 (1995).
7. J. N. Balaraju, T. S. N. S. Narayanan, and S. K. Seshadri, *J. Appl. Electrochem.*, **33**, 807 (2003).
8. J. Chitty, A. Pertuz, H. Hintermann, M. H. Staia, and E. S. Puchi, *Thin Solid Films*, **308–309**, 430 (1997).
9. H. Matsubara and A. Yamada, *J. Electrochem. Soc.*, **141**, 2386 (1994).
10. G. J. Lu and G. Zangari, *Electrochim. Acta*, **47**, 2969 (2002).
11. H. Knauss, B. Terheiden, and P. Fath, *Sol. Energy Mater. Sol. Cells*, **90**, 3232 (2006).
12. M. Yoshino, Y. Nonaka, J. Sasano, I. Matsuda, Y. Shacham-Diamand, and T. Osaka, *Electrochim. Acta*, **51**, 916 (2005).
13. S. Sabharwal, S. Palit, R. B. Tokas, A. K. Poswal, and Sangeeta, *Bull. Mater. Sci.* **31**, 729 (2008).
14. A. Duhin, Y. Sverdlov, I. Torchinsky, Y. Feldman, and Y. Shacham-Diamand, *Microelectron. Eng.*, **84**, 2506 (2007).
15. J. W. Yoon, J. H. Park, C. C. Shur, and S. B. Jung, *Microelectron. Eng.*, **84**, 2552 (2007).
16. Y. M. Chow, W. M. Lau, and Z. S. Karim, *Surf. Interface Anal.*, **31**, 321 (2001).
17. J. W. Yoon, J. M. Koo, J. W. Kim, S. S. Ha, B. I. Noh, C. Y. Lee, J. H. Park, C. C. Shur, and S. B. Jung, *J. Alloys Compd.*, **466**, 73 (2008).
18. S. Haag, M. Burgard, and B. Ernst, *Surf. Coat. Technol.*, **201**, 2166 (2006).
19. S. Yae, K. Ito, T. Hamada, N. Fukumuro, and H. Matsuda, *Plat. Surf. Finish.*, **92**, 58 (2005).
20. Y. L. Chang, W. C. Ye, C. L. Ma, and C. M. Wang, *J. Electrochem. Soc.*, **153**, C677 (2006).
21. S. L. Cheng and W. C. Hsiao, *Electrochem. Solid-State Lett.*, **10**, D142 (2007).
22. L. Y. Bai, F. L. Yuan, and Q. Tang, *Mater. Lett.*, **62**, 2267 (2008).
23. B. K. R. Nair, J. Choi, and M. P. Harold, *J. Membr. Sci.*, **288**, 67 (2007).
24. W. L. Liu, S. H. Hsieh, T. K. Tsai, W. J. Chen, and S. S. Wu, *Thin Solid Films*, **510**, 102 (2006).
25. W. L. Liu, S. H. Hsieh, and W. J. Chen, *J. Electrochem. Soc.*, **155**, D192 (2008).
26. S. Wehner, A. Bund, U. Lichtenstein, W. Plieth, W. Dahms, and W. Richtering, *J. Appl. Electrochem.*, **33**, 457 (2003).